6th International Conference on Advances in Experimental Structural Engineering
11th International Workshop on Advanced Smart Materials and Smart Structures Technology
August 1-2, 2015, University of Illinois, Urbana-Champaign, United States

Aerodynamic Control of Wind-Induced Vibrations and Flow Around Super-Tall Buildings

Y. Tamura[1], H. Tanaka[2], K. Ohtake[3], Y.C. Kim[4], A. Yoshida[5], E.K. Bandi[6], X. Xu[7], Q. Yang[8]

1 *Professor, School of Civil Engineering, Beijing jiaotong University, Beijing, China.*
Program Coordinator, Wind Engineering Research Center, Tokyo Polytechnic University, Kanagawa, Japan.
E-mail: yukio@arch.t-kougei.ac.jp
2 *Associate Chief Researcher, Takenaka Corporation, Chiba, Japan..*
E-mail: tanaka.hideyuki@takenaka.co.jp
3 *Chief Researcher, Takenaka Corporation, Chiba, Japan..*
E-mail: ohtake.kazuo@takenaka.co.jp
4 *Associate Professor, Wind Engineering Research Center, Tokyo Polytechnic University, Kanagawa, Japan.*
E-mail: kimyc@arch.t-kougei.ac.jp
5 *Professor, Wind Engineering Research Center, Tokyo Polytechnic University, Kanagawa, Japan.*
E-mail: yoshida@arch.t-kougei.ac.jp
6 *Professor, Madanapalle Institute of Technology and Science (MITS), Chittoor (Dt), Andhra Pradesh, India.*
E-mail: yoshida@arch.t-kougei.ac.jp
7 *PhD Candidate, Beijing Jiaotong University, Beijing, China.*
E-mail: 758229200@qq.com
8 *Professor, Beijing Jiaotong University, Beijing, China.*
E-mail: qshyang@bjtu.edu.cn

ABSTRACT
Tall buildings have been traditionally designed to be symmetric rectangular, triangular or circular in plan, in order to avoid excessive seismic-induced torsional vibrations. However, recent tall building design has been released from the spell of compulsory symmetric shape design, and this is mainly due to architects and structural designer's challenging demands for atypical expressions. One important aspect is that rather complicated sectional shapes show basically excellent aerodynamic performance. A series of wind tunnel tests have been carried out to determine wind forces and wind pressures acting on 45 tall building models with various configurations: square plan, rectangular plan, elliptic plan, with corner cut, with corner chamfered, tilted, tapered, inverse tapered, with setbacks, helical, openings and so on. Dynamic wind-induced response analyses of these models have also been conducted. Another important aspect in tall-building design and construction is induced environmental problems, especially pedestrian-level winds around buildings and assessment. A series of wind tunnel tests have also been conducted for the above mentioned building models to compare wind speed characteristics. The results of these tests have led to comprehensive discussions on the aerodynamic and flow characteristics of various tall building configurations, and studies on corresponding optimal structural systems.

KEYWORDS: *Tall buildings, Wind tunnel test, Wind-induced responses, Pedestrian-level wind.*

1. INTRODUCTION

The current tallest building in the world is the 828m-high Burj Khalifa, and the tallest building in the next decade will be Kingdom Tower (over 1000m), which will be completed in 2018, making Burj Khalifa the third tallest. According to a report [1] that examined world skyscrapers under construction as of January 2010, 56% of those within the top 100 highest buildings had been completed since 2000, and many tall buildings higher than 600m are still under construction. This trend of Manhattanization requires attention, particularly the preference for free-style building shapes, which are seen in Burj Kalifa and Shanghai Tower, presently under construction. Tall buildings have been traditionally designed to be symmetric rectangular, triangular or circular in plan, in order to avoid excessive seismic-induced torsional vibrations due to eccentricity. However, freewheeling building shapes have advantages not only in architectural design reflecting architects' challenging spirits for new forms but also in structural design reducing wind loads. Development of analytical techniques and of vibration control techniques has greatly contributed to this trend. In particular, across-wind response, which is a major factor in safety and habitability of tall buildings, is greatly suppressed.
The effectiveness of aerodynamic modification to reduce wind loads has been widely reported ([2] ~ [10]). However, most of the above papers have focused on the effect of one or two aerodynamic modifications that

change systematically. None have comprehensively investigated aerodynamic characteristics of various types of tall buildings with different configurations.

The authors' group has conducted wind tunnel experiments for the super-tall buildings with unconventional configurations to investigate the aerodynamic and response characteristics. The findings can provide the structural designer with comprehensive wind tunnel test data that can be used in the preliminary design stage, and can be helpful in evaluating the most effective structural shape in wind-resistant design for tall buildings with various aerodynamic modifications.

2. WIND TUNNEL TEST

2.1. Configurations of Super-Tall Buildings

The super-tall building models used for the experiments are shown in Table 1. The full-scale height and the total volume of each building model are commonly set at H = 400m (80 stories) and 10^6 m^3. The width B of the Square model shown in Table 1(a) is 50m and the aspect ratio H/B is 8. The geometric scale of the wind tunnel models is set at 1/1000. The tall building models examined in this study are classified into 9 categories as follows.

Table 2.1 Configurations of super-tall building models

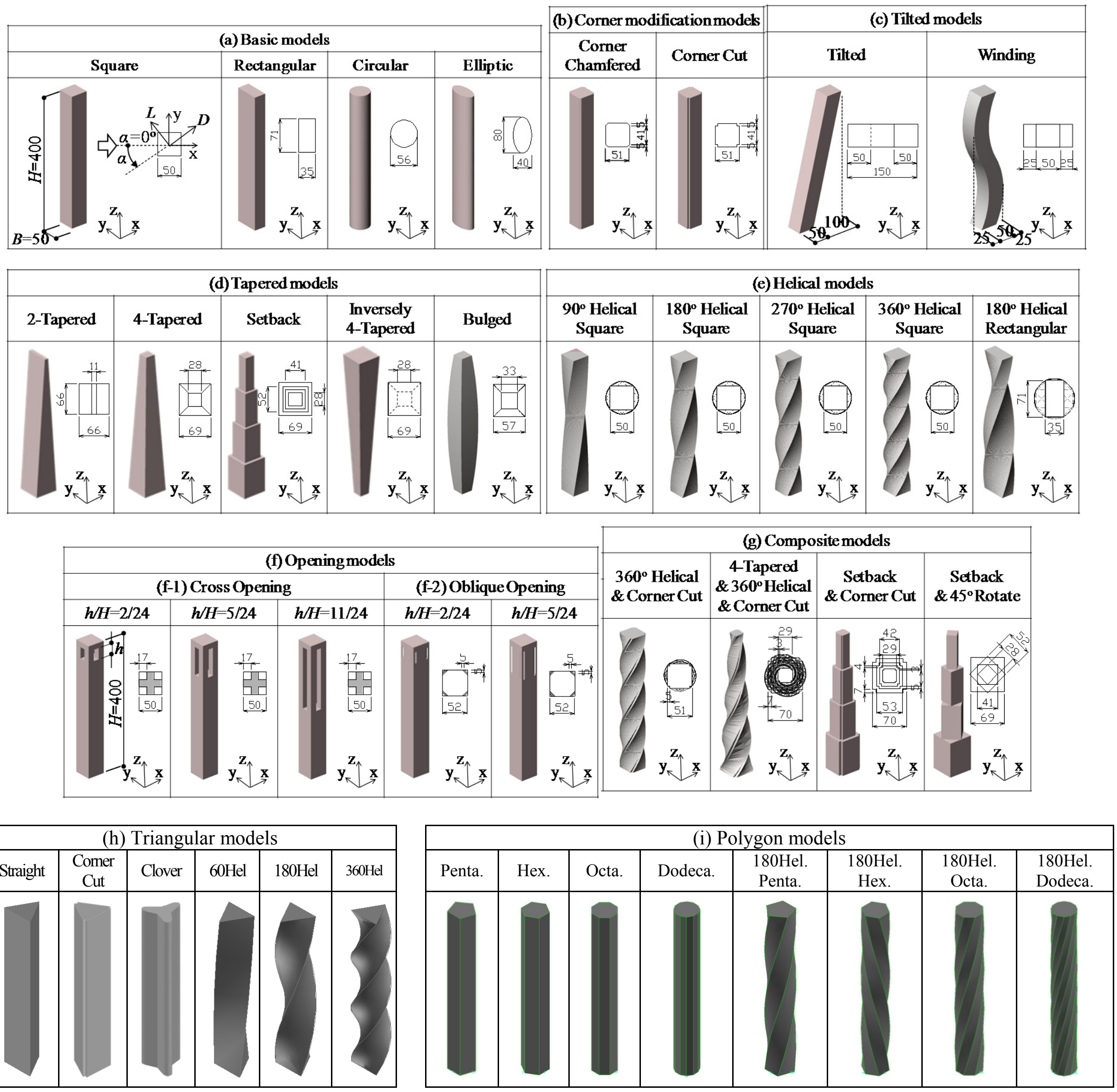

2.2. Experimental Conditions

Wind tunnel experiments were performed in a closed-circuit-type boundary-layer wind tunnel whose working section is 1.8m high by 2.0m wide. Fig. 2.1 shows the condition of the approaching turbulent boundary layer flow with a power-law index of 0.27, representing an urban area. The wind velocity and turbulence intensity at the top of the model were about U_H=7.0m/s and I_{UH}=9.2%, respectively. The turbulence scale near the model top was about 0.360m, and that of AIJ-RLB (2004) is 365m [11]. Therefore, when considering the length scale of 1/1000, the flow conditions of the present work are thought to be appropriately simulated. Dynamic wind forces were measured by a 6-component high-frequency force balance (HFFB) supporting light-weight and stiff models. Wind direction α was changed from 0°, which is normal to a wall surface, to 45° or 180° every 5° depending upon the building configuration. The measured wind forces and aerodynamic moments are normalized by $q_H BH$ and $q_H BH^2$ to get wind force coefficients and moment coefficients, respectively. Here, q_H is the velocity pressure at the model height H, and B is commonly set at the width of the Square Model. Thus, the force and moment coefficients of the models can be directly compared. Fig. 2.2 shows the definitions of wind forces, moments, and the coordinate system employed in this study.

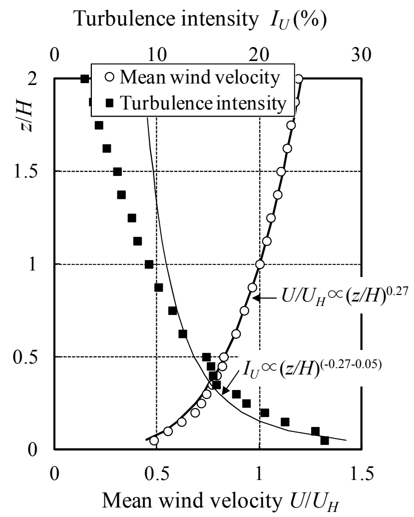

Figure 2.1 Flow conditions of wind tunnel test

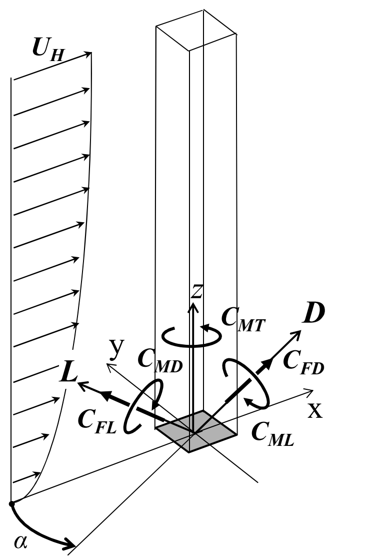

Figure 2.2 Coordinate system

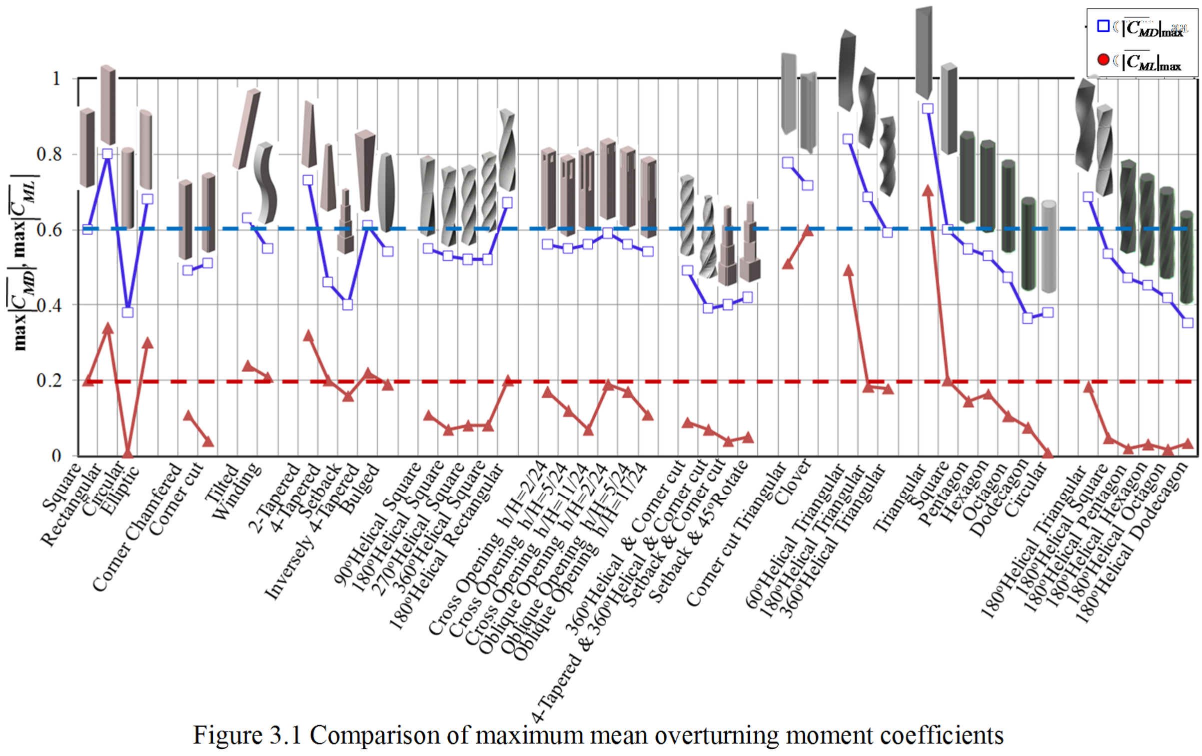

Figure 3.1 Comparison of maximum mean overturning moment coefficients

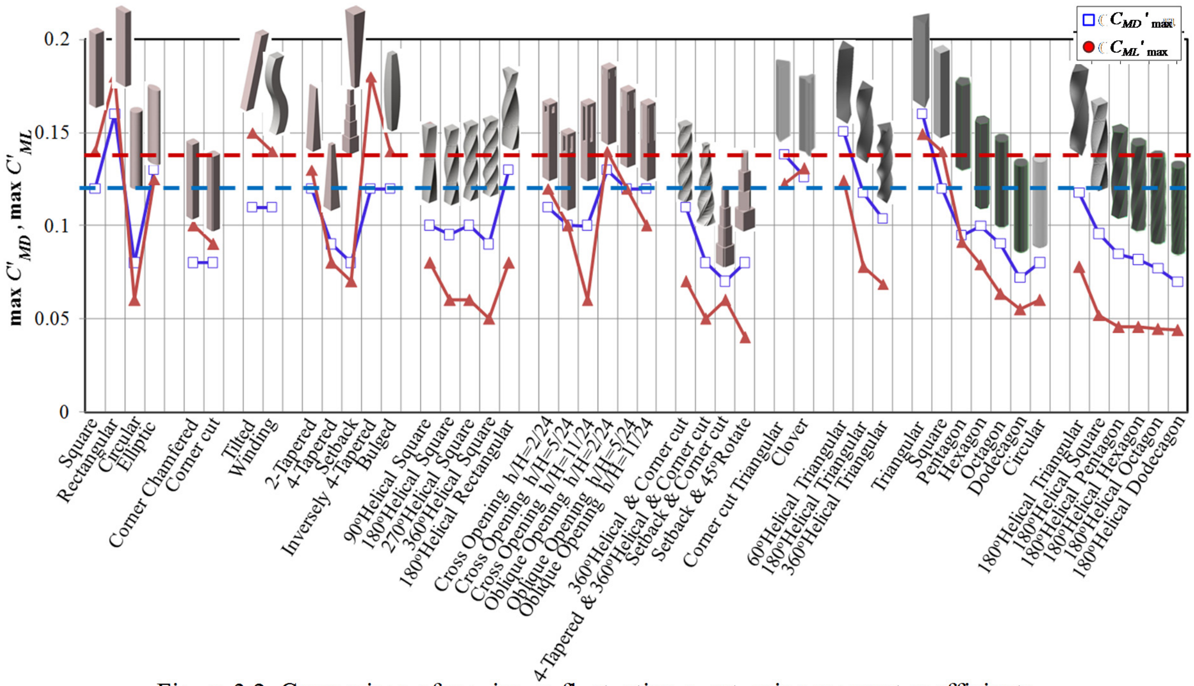

Figure 3.2. Comparison of maximum fluctuating overturning moment coefficients

Wind pressure measurements were conducted on 28 models. They were determined from the results of aerodynamic force measurements and for relatively realistic building shapes in the current era. The aims of the pressure measurements were to examine the characteristics of local wind forces and aerodynamic phenomena in detail. In addition, response analyses were conducted using the results of the pressure measurement.

The coordinate system and approaching flow for the wind pressure measurements are the same as for the aerodynamic force measurement (see Fig. 2.1 and Fig. 2.2), except that the wind velocity at model height was 11.8m/s. Also, the wind direction was changed from 0° to 355° at 5° intervals as for the aerodynamic force measurements. The fluctuating wind pressures of each pressure tap were measured and recorded simultaneously using a vinyl tube 80cm long through a synchronous multi-pressure sensing system (SMPSS). The sampling frequency was 1kHz with a low-pass filter of 500Hz. The total number of data was 32,768. The fluctuating wind pressures were revised considering the transfer function of the vinyl tube. There were about 20 measurement points on one level on four surfaces, and the measurement points were instrumented at 10 levels (12 levels only for Setback model), giving more than 200 measurement points. The wind pressure coefficients C_p were obtained by normalizing the fluctuating pressures by the velocity pressure q_H at model height. The local wind force coefficients, C_{fD} for along-wind, C_{fL} for crosswind and C_{mT} for torsional moment, were derived by integrating the wind pressure coefficients C_p using the building width B of the Square Model (B^2 for torsional moment) regardless of building shape.

3. RESULTS AND DISSCUSSION

3.1. Overturning Moment Coefficients

Fig. 3.2 shows the maximum values of the mean along- and across-wind o.t.m. coefficients, $|\overline{C_{MD}}|_{max}$ and $|\overline{C_{ML}}|_{max}$ considering all wind directions. The maximum along-wind o.t.m. coefficient $|\overline{C_{MD}}|_{max}$ and across-wind o.t.m. coefficient $|\overline{C_{ML}}|_{max}$ of the Circular model is smallest among all experimental models, and those of the Rectangular model, the Triangular and Elliptic models are larger than those of the Square model because of their larger widths. The maximum mean along-wind o.t.m. coefficients $|\overline{C_{MD}}|_{max}$ of the 4-Tapered model and the Setback model, whose sectional area decreases with height, are relatively small. However, for the three Cross Opening models, whose projected areas also decrease at their upper parts, the maximum mean along-wind o.t.m. coefficient $|\overline{C_{MD}}|_{max}$ does not decrease as much as those of the 4-Tapered and the Setback models. This may be because of the reduced effectiveness of the openings as the wind direction approaches 45°. The maximum mean across-wind o.t.m. coefficients $|\overline{C_{ML}}|_{max}$ of the Corner Cut and Corner Chamfered models are small. The maximum mean across-wind o.t.m. coefficients of the Helical Square and the Cross Opening h/H=11/24 models whose opening size is the largest are also small. The small coefficients of those models are related to vortex formation and shedding. Conversely, the models whose along- and across-wind o.t.m. coefficients are larger than those of the Square model are the 2-Tapered, the 180° Helical Rectangular and the Tilted models with larger projected area for a certain wind direction, and the Inversely 4-Tapered model with larger projected area at its upper height. The maximum mean o.t.m. coefficients $|\overline{C_{MD}}|_{max}$ and $|\overline{C_{ML}}|_{max}$ of a Helical Square/Triangular model with a larger helical angle tends to show smaller values. And the variations of mean o.t.m. coefficients $\overline{C_{MD}}$ and $\overline{C_{ML}}$ of the 90°Helical Square and 180°Helical Square models with wind direction are very small. In particular, the 180°Helical Square model shows values almost independent of wind direction. For the opening models, as the opening size h/H becomes larger, the maximum mean o.t.m. coefficient $|\overline{C_{ML}}|_{max}$ decreases. However, the decreasing tendency is not significant for the maximum mean across-wind coefficient $|\overline{C_{MD}}|_{max}$ for both the Cross Opening and the Oblique Opening models. The aerodynamic characteristics of the composite models with multiple modifications are mostly superior to those of the models with single modification. However, note that the mean o.t.m coefficients of the 360° Helical + Corner-cut model are almost the same as those of the 360° Helical model, implying that the aerodynamic characteristics have not been further improved by corner modification.

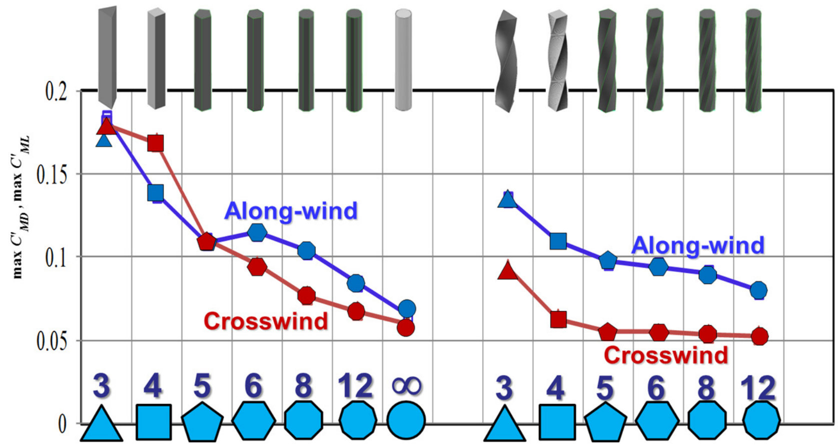

(a) Straight model (b) 180°Helical model

Figure 3.3. Comparison of maximum fluctuating overturning moment coefficients of polygon models

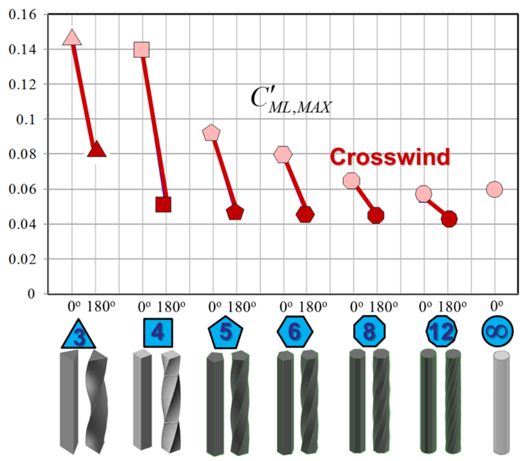

Figure 3.4. Effect of helical shape on maximum fluctuating overturning moment coefficients

Fig. 3.2 shows the maximum along-wind and across-wind fluctuating o.t.m. coefficients, $C_{MD}'{}_{max}$ and $C_{ML}'{}_{max}$, considering all wind directions. The maximum fluctuating along-wind o.t.m. coefficients $C_{MD}'{}_{max}$ of the Corner Chamfered, Corner Cut, 4-Tapered and Setback models are smaller. The maximum fluctuating across-wind o.t.m. coefficients $C_{ML}'{}_{max}$ of the 4-Tapered, Setback, Helical Square, and Cross Opening 11/24 models show relatively small values. Detailed aerodynamic phenomena will be discussed later. These trends are the same as those of the maximum mean o.t.m. coefficients. And, the effect of helical angle θ for the Helical Square models, the effects of opening size for the two types of Opening models, and the composite effect also show the same tendency as those of the maximum mean o.t.m. coefficients.

Fig. 3.3 compares the maximum fluctuating overturning moment coefficients of polygon models. For the straight model, they decrease with increasing number of sides, even when the number of side is larger than 12. But for the helical models, they show similar values for the polygon models when the number of sides is larger than 5. The effect of helical shape on the maximum fluctuating overturning moment coefficients is shown in Fig. 3.4. Large suppression is shown for the square model, but the degree of suppression become smaller with increasing number of sides.

3.2. Power spectral densities of crosswind overturning moment coefficients

Fig. 3.5 shows a detailed comparison of the square root of the power spectra for the design wind speed corresponding to 500- and 1-year return periods. The design wind speeds in Tokyo for the corresponding return periods are assumed to be $V_{p,500}$=71m/s and $V_{p,1}$=30m/s, respectively. The values for the Corner Cut, Tapered, Setback, Helical Square (θ=180º~360º), and Cross Opening (h/H=11/24) models are almost one third or one fourth that of the Square model, showing advantages for safety design (Fig. 8(a)). And the values for the Corner cut + 4-Tapered + 360ºHelical Square and Setback + 45ºRotate models are almost one tenth that of the Square model, so it can be said that the Combination models are very effective building shapes for safety design. The spectral values corresponding to a 1-year return period for the Tilted, Tapered and Oblique Opening models (Fig. 8(b)) are generally large, and even for the 4-Tapered and Setback model, the values are larger than that for the Square model. But the values for the Corner cut, Helical Square (θ=180º~360º), and Cross Opening (h/H=11/24) are smaller than that for the Square model, meaning that these building shapes are superior to the Square model from the viewpoint of habitability design. For all the composite models, the values become smaller than that for the Square model.

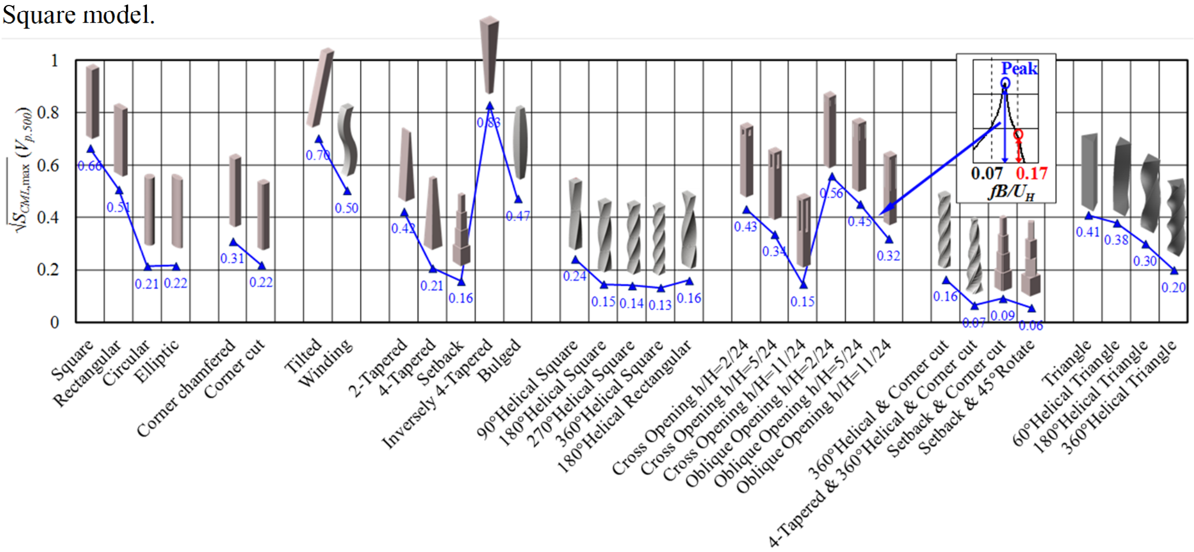

(a) Spectral values for $V_{p,500}$

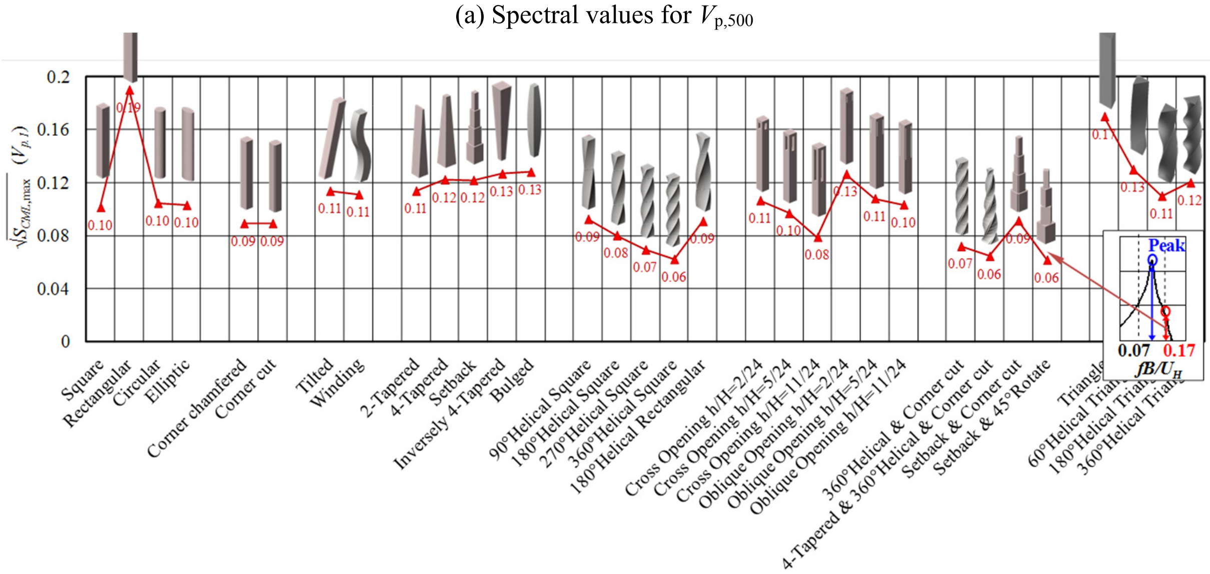

(b) Spectral values for $V_{p,1}$

Figure 3.5 Power spectral density of crosswind direction and spectral values

3.3. Response Analyses

The maximum acceleration and maximum displacement of some selected models are shown in Fig. 3.6. All maximum values in Fig. 3.6 are shown as their ratios to that of the Square model. The single modification models that show that smaller responses for all items are Corner Cut, Corner Chamfered, 90°Helical and 180°Helical. For the 4-Tapered, Setback, and Cross Opening, the maximum acceleration is larger than that of the Square model. All composite models show smaller values for all items. When comparing the 4-Tapered + 180° Helical model with the 4-Tapered model with the same structural characteristics, the suppression of response is significant. It was found that there is little difference for maximum displacement and acceleration for two composite models with different helical angles of 4-Tapered + 180°Helical + Corner Cut model and 4-Tapered + 360°Helical + Corner Cut model (not shown in Fig. 3.6), implying that the helical angle of 180° is enough.

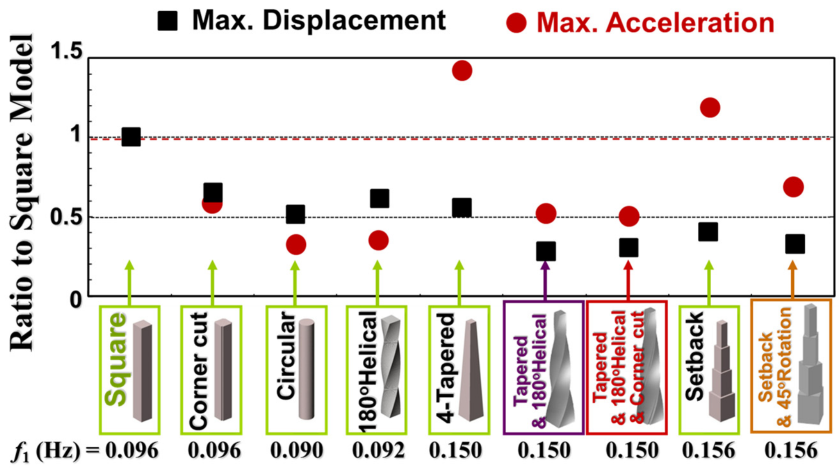

Figure 3.6. Comparison of wind-induced responses for 500-year return period design wind speed

4. PEDESTRIAN LEVEL FLOW

Pedestrian level flow conditions were examined using larger models than those of the pressure measurement and force balance test. The width of the square model was 10cm, and the aspect ratio was 1/8. Thermistor sensors were used to measure the wind velocity at 5mm height around the buildings (full-scale: 2.5m). The measurement area was 396mm^2 in model scale. Because the wind speed changed significantly in the area near the building, the sensors were concentrated in the central area around the building. The minimum distance between two sensors was 2cm, and the maximum distance in the outside area was 8cm.

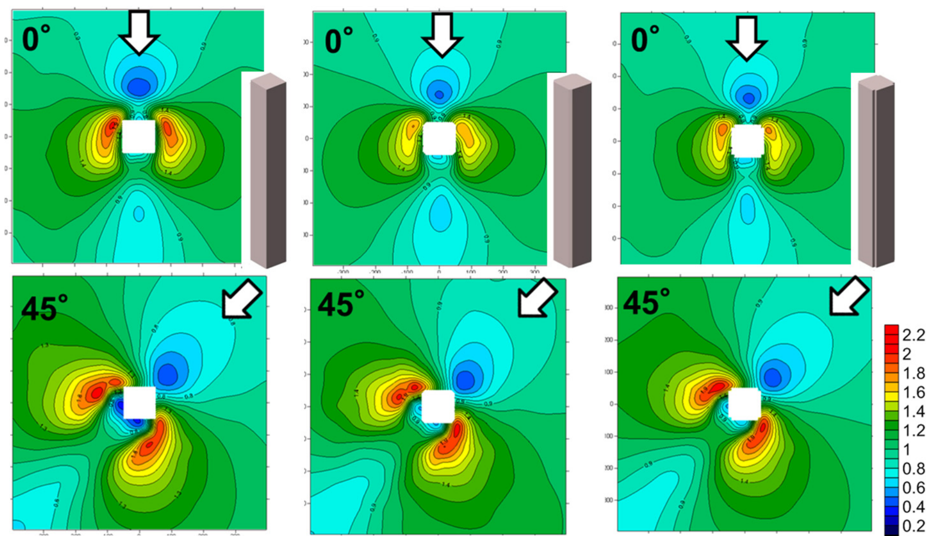

(a) Square model (b) Corner Chamfered model (c) Corner Cut model

Figure 4.1 Pedestrian level flow environment

The features of the mean wind speed distributions around the square model and two corner modification models are shown in Fig.4.1. It can see that, compared with the square model, the wind speed ratio of the corner modification models are significantly reduced. The maximum wind speed ratio of the square model is 2.2. The wind speed ratio of the corner cut model and the corner chamfered model are 2.0 and 1.9, respectively.

5. CONCLUDING REMARKS

For the super-tall building models with various building shapes and the same height and volume, the aerodynamic force measurements, wind pressure measurements and pedestrian level flow measurements were conducted. Comparison and discussion of the aerodynamic and response characteristics of super-tall buildings led to the following conclusions.

1. For the maximum mean overturning moment coefficients, 4-Tapered and Setback models show better aerodynamic behaviors in the along-wind direction, and Corner modification models, Helical models, and Cross Opening models with h/H=11/24 show better aerodynamic behaviors in the across-wind direction.
2. For the maximum fluctuating overturning coefficients, the Corner Modification, 4-Tapered and Setback models show better aerodynamic behaviors in both along-wind and across-wind directions. The Cross Opening model with h/H=11/24 and the Helical models also show better aerodynamic behaviors in the across-wind direction.
3. The aerodynamic characteristics of the composite models with multiple modifications are mostly superior to those of the models with single modification.
4. By introducing the corner modifications, the pedestrian level flow environment was improved.
5. Evaluations of aerodynamic and response characteristics depending on building shapes are indispensable in super-tall building projects, prior to planning the vibration control systems for super-tall buildings

AKCNOWLEDGEMENT

N. Koshika of Kajima Corp., K. Yamawaki of Nikken Sekkei Ltd., Y. Hitomi of Nihon Sekkei Ltd., Y. Hayano of MAD Tokyo and S. Igarashi of Takenaka Corp. provided us with helpful advices for setting experimental cases. This study was partially funded by the Ministry of Land, Infrastructure, Transport and Tourism, Japan.

REFERENCES

1. Tamura Y., Nakai M., Ohtake K., Koshika K., Yamawaki K., Hitomi K. (2011). Study on wind resistant design method of super high-rise buildings with various unconventional configurations. The Ministry of Land, Infrastructure, Transport and Tourism. Tokyo, Japan (in Japanese).
2. Bandi E.K., Tamura Y., Yoshida A., Kim Y.C., Yang Q. (2012). Local and total wind force characteristics of triangular-section tall buildings. *Proceedings of the 22nd National Symposium on Wind Engineering*. Tokyo, Japan.
3. Cooper K.R., Nakayama M., Sasaki Y., Fediw A.A., Resende-Ide S., Zan S.J. (1997). Unsteady aerodynamic force measurements on a super-tall building with a tapered cross section. *Journal of Wind Engineering and Industrial Aerodynamics*. **72**, 199-212.
4. Kawai H. (1998). Effect of corner modifications on aeroelastic instabilities of tall buildings. *Journal of Wind Engineering and Industrial Aerodynamics*. **74-76**, 719-729.
5. Kim Y.C., Kanda J. (2010). Characteristics of aerodynamic forces and pressures on square plan buildings with height variations. *Journal of Wind Engineering and Industrial Aerodynamics*. **98**, 449-465.
6. Kim Y.C., Kanda J. (2013). Wind pressures on tapered and set-back tall building. *Journal of Fluids and Structures.* **39**, 306-321.
7. Kim Y.C., Kanda J., Tamura Y. (2011). Wind-induced coupled motion of tall buildings with varying square plan with height. *Journal of Wind Engineering and Industrial Aerodynamics*. **99:5**, 638-650.
8. Kim Y.C., Tamura Y., Tanaka H., Ohtake K., Bandi E.K., Yoshida A. (2013). Aerodynamic characteristics of tall buildings with unconventional configurations. *12th Americas Conference on Wind Engineering*, Seattle, Washington, USA.
9. Tanaka H., Tamura Y., Ohtake K., Nakai M., Kim Y.C. (2012). Experimental investigation of aerodynamic forces and wind pressures acting on tall buildings with various unconventional configurations. *Journal of Wind Engineering and Industrial Aerodynamics.* **107-108**, 179-191.
10. Tanaka H., Tamura Y., Ohtake K., Nakai M., Kim Y.C. (2013). Aerodynamic and flow characteristics of tall Buildings with various unconventional configurations. *International Journal of High-Rise Buildings*. **2:3**, 213-228.
11. Architectural Institution of Japan. (2004). Recommendations for loads on buildings (2004). Architectural Institution of Japan, Tokyo.